

## Synthesis and biological studies of nanostructured metal coordination polymers derived from 1,3-di(4-pyridyl)-propane and 1-methylimidazole

Aref A.M.Aly\*, Maged S.Al-Fakeh, Mahmoud A.Ghandour, Bahaa M.Abu-Zied  
Department of Chemistry, Faculty of Science, Assiut University, 71516 Assiut, (EGYPT)  
E-mail : aref\_20002001@yahoo.com; maged7969@yahoo.com

### ABSTRACT

A series of coordination polymers of the general formula  $\{[M(DPP)(MIMZ)X(H_2O)]_n \cdot xH_2O\}$ , (M = Mn(II), Co(II), Cu(II), Cd(II) and Pb(II), DPP = 1,3-di(4-pyridyl)propane and MIMZ = 1-methylimidazole, X = chloride or nitrate, has been prepared and characterized. The structure of the coordination polymers has been assigned based on elemental analysis, FT-IR and electronic spectral studies, thermal analysis, scanning electron microscope (SEM) and X-ray powder diffraction. Thermogravimetric analysis (TGA) was also used to follow up the possible thermal decomposition steps and to calculate the thermodynamic parameters of the nano-sized metal complexes. The kinetic parameters have been calculated making use of the Coats-Redfern and Horowitz-Metzger equations. The antimicrobial activity of the synthesized compounds was tested against six fungal and five bacterial species.

© 2013 Trade Science Inc. - INDIA

### KEYWORDS

Nano-sized coordination;  
Thermal studies;  
Biological activity.

### INTRODUCTION

Coordination polymers span scientific fields such as organic and inorganic chemistry, biology, materials science, electrochemistry, and pharmacology, having many potential applications<sup>[1-5]</sup>. They represent an important interface between synthetic chemistry and material science. Nanometer-sized particles of metal coordination polymers are of interest to explore, since their unique properties are controlled by the large number of surface molecules, leading to an entirely different environment than those in a bulk crystal<sup>[6]</sup>. The flexible nitrogen donor ligand 1,3-di(4-pyridyl)propane is used in the construction of coordination polymers that can show a wide range of interesting topologies as chains, ladders, grids and

adamantoid networks<sup>[7,8]</sup>. 1-Methylimidazole and its derivatives have been used to mimic aspects of these biomolecules. MIMZ is also the precursor for the synthesis of the methylimidazole monomer of pyrrole-imidazole polyamides. These polymers can selectively bind specific sequences of double-stranded DNA by intercalating in a sequence dependent manner<sup>[9]</sup>. Imidazole and its derivatives represent a very interesting class of compounds because of their pharmaceutical, analytical, most common binding sites in various metalloenzymes and industrial applications<sup>[10-12]</sup>. We report in this work on the synthesis and characterization of manganese(II), cobalt(II), copper(II), cadmium(II) and lead(II) coordination polymers with DPP and MIMZ. The structures of the ligands are presented in Figure 1.

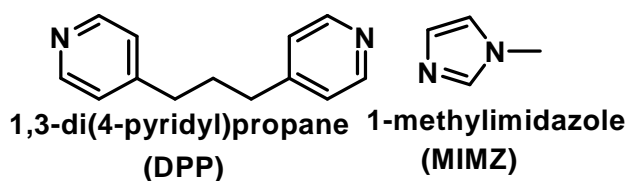


Figure 1 : Chemical structure of DPP and MIMZ

## EXPERIMENTAL

### Materials and methods

All chemicals used were of analytical grade. High purity 1,3-di (4-pyridyl)propane and 1-methylimidazole were supplied from Sigma Aldrich and E. Merck grad respectively. All other metal salts chemicals were of AR grade. They were purchased and used without purification.

### Preparation of the coordination polymers

Preparation of Mn(II), Co(II), Cu(II), Cd(II) and Pb(II) mixed ligand coordination polymers of 1,3-di (4-pyridyl)propane and 1-methylimidazole follows essentially the same procedure.  $[\text{Cu}(\text{DPP})(\text{MIMZ})\text{Cl}_2(\text{H}_2\text{O})_n]_n$  synthesis is typical. An ethanolic solution 15 mL of DPP (1.5 mmol) was slowly added into a hot ethanolic solution (15 mL) of  $\text{CuCl}_2 \cdot 2\text{H}_2\text{O}$  (1.5 mmol) and to an aqueous solution of MIMZ (1.5 mmol) was added dropwise. The resultant mixture was stirred for 1 h and filtered. The Light-green precipitate was separated, washed with distilled water and EtOH and then dried over  $\text{CaCl}_2$  in a vacuumed desiccator.

### Physical measurements

The stoichiometric analyses (C,H,N) were performed using Analyischer Funktionstest Vario El Fab-Nr.11982027 elemental analyzer. The conductance was measured using a conductivity Meter model 4310 JENWAY. The i.r spectra were recorded on a Shimadzu IR-470 spectrophotometer and the electronic spectra were obtained using a Shimadzu UV-2101 PC spectrophotometer. Thermal studies were carried out in dynamic air on a Shimadzu DTG 60-H thermal analyzer at a heating rate  $10^\circ\text{C min}^{-1}$ . The X-ray diffractometer was a Philips 1700 version with H. T. P.W 1730 / 104 KVA and the anode was Cu  $K\alpha$  ( $\lambda = 1.54180 \text{ \AA}$ ). The scanning electron microscope was a JEOL JFC-1100E ION SPUTTERING DEVICE, JEOL JSM-5400LV.

SEM specimens were coated with gold to increase the conductivity.

### Biological activity

The antimicrobial activity of the complexes was tested against 5 bacterial and 6 fungal strains. These strains are common contaminants of the environment in Egypt and some of which are involved in human and animal diseases (*Candida albicans*, *Geotrichum candidum*, *Scopulariopsis brevicaulis*, *Aspergillus flavus*, *T. rubrum*, *Staphylococcus aureus*), plant diseases (*Fusarium oxysporum*) or frequently reported from contaminated soil, water and food substances (*Escherichia coli*, *Bacillus cereus*, *Pseudomonas aeruginosa* and *Serratia marcescens*). To prepare inocula for bioassay, bacterial strains were individually cultured for 48h in 100 ml conical flasks containing 30 ml nutrient broth medium. Fungi were grown for 7 days in 100 ml conicals containing 30 ml Sabouraud's dextrose broth. Bioassay was done in 10 cm sterile plastic Petri plates in which microbial suspension (1 ml/plate) and 15 ml appropriate agar medium (15 ml/plate) were poured. Nutrient agar and Sabouraud's dextrose agar were respectively used for bacteria and fungi. After solidification of the media, 5 mm diameter cavities were cut in the solidified agar (4 cavities/plate) using sterile cork borer. The chemical compounds dissolved in dimethyl sulfuxide (DMSO) at 2% w/v (=20 mg/ml) were pipetted in the cavities (20 ul /cavity). Cultures were then incubated at  $28^\circ\text{C}$  for 48 h in case of bacteria and up to 7 days in case of fungi. The results were read as the diameter (in mm) of inhibition zone around cavities.

## RESULTS AND DISCUSSION

The coordination polymers were prepared by the reaction of DPP, metal chlorides or nitrate, and MIMZ (dissolved in EtOH). The prepared compounds were found to react in the molar ratio 1: 1: 1 metal : DPP : MIMZ. The complexes are air stable, insoluble in common organic solvents but partially soluble in DMSO. The corresponding complexes are obtained according to the equations:



M = Mn(II), Co (II), Cu (II) or Cd(II), x = 0 or 2.

## Full Paper



The results are listed in TABLE 1 together with the color and melting points of the complexes.

### IR spectra

The infrared spectra of compounds (Figure 2) show a number of bands at 1610, 1611, 1616, 1608 and 1606  $\text{cm}^{-1}$  corresponding to  $\nu(\text{C}=\text{N})$  1,3-(4-pyridyl)propane for manganese(II), cobalt(II), copper(II), cadmium(II) and lead(II) complexes respectively<sup>[13]</sup>. The i.r. spectra for the complexes show a series of bands at 803, 807, 822, 825 and 812  $\text{cm}^{-1}$  corresponding to the coordination of  $\nu(\text{C}-\text{N})$  1-methylimidazole moieties<sup>[14]</sup>. A band was found in the

1355  $\text{cm}^{-1}$  region corresponding to the  $\nu(\text{NO}_3)$  of Pb(II) compound<sup>[15]</sup>. The M-O and M-N bonding are manifested by the appearance of two bands at 430-454  $\text{cm}^{-1}$  and 512-530  $\text{cm}^{-1}$  regions, respectively<sup>[16]</sup>. The stretching vibration of  $\nu\text{OH}$  of coordinated water is located in the region 3125-3356  $\text{cm}^{-1}$ <sup>[17]</sup> for all the complexes. For the Cd(II) compound,  $\nu\text{OH}$  stretching vibration of lattice water was observed in the 3430  $\text{cm}^{-1}$ <sup>[18]</sup>. The results are given in TABLE 2.

### Electronic spectra and magnetic moments

The band observed in the electronic spectra (in DMSO) of the Mn (II), Co (II), Cu (II), Cd (II) and Pb (II) ternary coordination polymers of 1,3-(4-pyridyl)

TABLE 1 : Colors, elemental analysis and melting points of the compounds

Compound	M. F (M.Wt)	Color	Found (Calcd. %)			m.p. °C (Decom.)	$\Lambda_m$ , Scm <sup>2</sup> mol <sup>-1</sup>
			C	H	N		
[Mn(DPP)(MIMZ)Cl <sub>2</sub> (H <sub>2</sub> O)] <sub>n</sub> 1	C <sub>17</sub> H <sub>22</sub> Cl <sub>2</sub> MnN <sub>4</sub> O (424.27)	Light-brown	49.34 48.12	5.50 5.23	12.96 13.20	210	51.70
[Co(DPP)(MIMZ)Cl <sub>2</sub> (H <sub>2</sub> O)] <sub>n</sub> 2	C <sub>17</sub> H <sub>22</sub> Cl <sub>2</sub> CoN <sub>4</sub> O (428.26)	Blue	48.23 47.67	5.52 5.18	12.03 13.08	234	46.23
[Cu(DPP)(MIMZ)Cl <sub>2</sub> (H <sub>2</sub> O)] <sub>n</sub> 3	C <sub>17</sub> H <sub>22</sub> Cl <sub>2</sub> CuN <sub>4</sub> O (432.88)	Light-green	48.03 47.16	5.23 5.13	12.10 12.94	200	30.89
{[Cd(DPP)(MIMZ)Cl <sub>2</sub> (H <sub>2</sub> O)].2H <sub>2</sub> O} <sub>n</sub> 4	C <sub>17</sub> H <sub>26</sub> Cl <sub>2</sub> CdN <sub>4</sub> O <sub>3</sub> (517.78)	White	40.19 39.43	5.35 5.07	9.87 10.82	227	39.86
[Pb(DPP)(MIMZ)(NO <sub>3</sub> ) <sub>2</sub> (H <sub>2</sub> O)] <sub>n</sub> 5	C <sub>17</sub> H <sub>22</sub> PbN <sub>6</sub> O <sub>7</sub> (629.65)	White	33.34 32.42	4.08 3.52	12.90 13.35	255	55.12

propane and 1-methylimidazole which located in the region 38,322-39,215  $\text{cm}^{-1}$  assigned to a  $\pi \rightarrow \pi^*$  transition due to molecular orbital energy levels originating in the DPP moiety. For all the complexes another band is recorded in the region 28,248-35,714  $\text{cm}^{-1}$  is ascribed to an intraligand transition for the MIMZ. For manganese complex the electronic spectra exhibit a band in the 20,181  $\text{cm}^{-1}$  reflecting the octahedral arrangement around the Mn(II) ion which is confirmed by the value of the magnetic moment (5.40 BM)<sup>[19]</sup>. Cobalt(II) compound a d-d band observed in the

22,123  $\text{cm}^{-1}$ . The corresponding magnetic moment value for this compound was found to be 4.33 BM, which is in agreement with the octahedral environment around Co(II) ion<sup>[20]</sup>. The magnetic moment value of 1.80 B.M for the Cu(II) complex indicates a octacoordination around copper(II) and a d-d band showed in the 19,920  $\text{cm}^{-1}$ <sup>[21]</sup>. The electronic spectral data and mag-

TABLE 2 : Infrared spectral data of the coordination polymers

Compounds	$\nu(\text{C}=\text{N})$	$\nu(\text{C}-\text{N})$	$\nu(\text{OH})\text{coord.}$	$\nu(\text{M}-\text{N})$	$\nu(\text{M}-\text{O})$
1	1610	803	3344	430	512
2	1611	807	3305	436	516
3	1616	822	3320	442	518
4	1608	825	3125	448	522
5	1606	812	3356	454	530

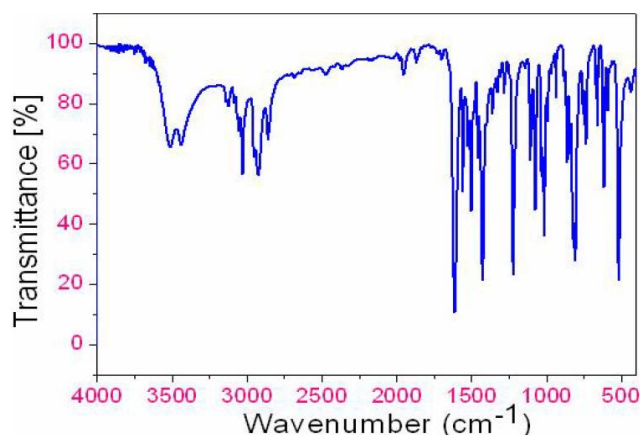


Figure 2 : FT-IR of compound Co(II) coordination polymer

netic moment values are shown in TABLE 3.

**TABLE 3 : Electronic spectral data and magnetic moments of the compounds**

Compound	$\nu_{\max}$ (cm <sup>-1</sup> )	Assignment	$\mu_{\text{eff}}$ B.M
1	20,181	d-d transition	5.40
	30,125	$n \rightarrow \pi^*$ transition	
	38,322	$\pi \rightarrow \pi^*$ transition	
2	22,123	d-d transition	4.33
	28,409	$n \rightarrow \pi^*$ transition	
	38,910	$\pi \rightarrow \pi^*$ transition	
3	19,920	d-d transition	1.80
	28,248	$n \rightarrow \pi^*$ transition	
	39,062	$\pi \rightarrow \pi^*$ transition	
4	35,714	$n \rightarrow \pi^*$ transition	-
	38,759	$\pi \rightarrow \pi^*$ transition	
5	35,460	$n \rightarrow \pi^*$ transition	-
	39,215	$\pi \rightarrow \pi^*$ transition	

The suggested structures for DPP mixed ligand coordination polymers are shown in Figures (3-4). It is to be noted that in all the published results of 1,3-di (4-pyridyl)propane the two pyridyl moieties stand almost cis to each other with different conformations and certain angle<sup>[22,23]</sup>.

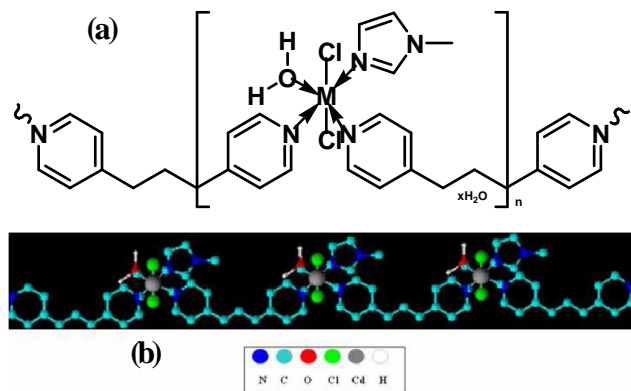


**Figure 3 : a) Structure of  $[[M(\text{DPP})(\text{MIMZ})\text{Cl}_2(\text{H}_2\text{O}) \cdot x\text{H}_2\text{O}]_n$ , (M = Mn(II), Co(II), Cu(II) and Cd(II), x = 0 or 2); b) A perspective view of the complete coordination around Cd(II)**

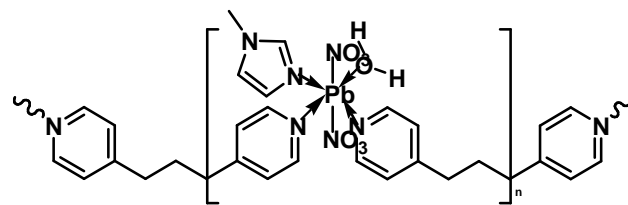


**Figure 4 : Structure of  $[\text{Pb}(\text{DPP})(\text{MIMZ})(\text{NO}_3)_2(\text{H}_2\text{O})]_n$**

### Thermal analysis

The thermal decomposition of compounds (2) and

(3) has been investigated in dynamic air from ambient temperature to 750 °C and the thermal data are cited in TABLE 4. As a representative, the thermogram of the Co (II) coordination polymer 2 is depicted in Figure 5. It shows four decomposition steps occurring in the temperature ranges 39-144, 145-283, 284-442 and 443-750 °C. The first one corresponds to the loss of the coordinated water molecule (calc. 4.20 %, found 3.32 %) (DTG peak at 76 °C), for which a broad endothermic peak appears in the DTA curve at 79 °C. The second mass loss is related to the free ligand of MIMZ (calc.19.17 %, found 20.69 %) (DTG peak at 245 °C). This step is marked on the DTA curve by a broad exothermic effect at 247 °C. The subsequent third and fourth steps are decomposition products of the remainder of the ligand. For these steps the DTG peaks appear at 320, 525 °C and two exothermic effects are recorded in the DTA trace at 322, 528 °C, respectively (calc. 62.85 %, found 59.77 %). The residue is assigned to be CoO as indicated from the mass loss (calc.17.49 %, found 16.22 %).

**TABLE 4: Thermal decomposition data of the compounds (2-3) in dynamic air**

Compound	Step	TG/DTG			Mass Loss(%)
		Ti	Tm	Tf	
2	1st	39	77	144	3.32
	2nd	145	245	283	20.69
	3rd	284	320	442	30.32
	4th	443	526	750	28.45
3	1st	43	77	145	5.66
	2nd	146	294	393	20.93
	3rd	394		750	56.90

Ti=Initial temperature, Tm=Maximum temperature, Tf=Final temperature

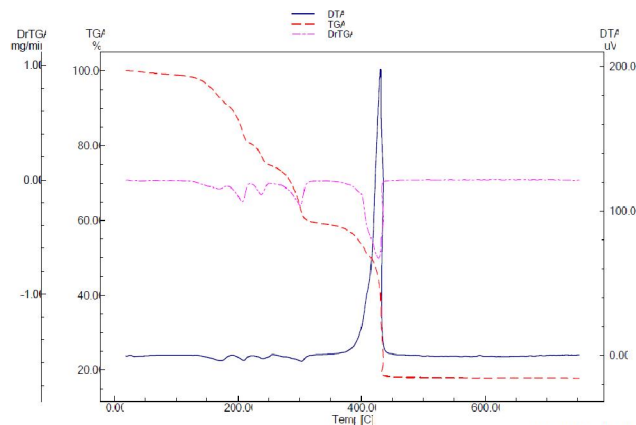


**Figure 5 : TG, DTG and DTA thermograms of  $[\text{Co}(\text{DPP})(\text{MIMZ})\text{Cl}_2(\text{H}_2\text{O})]$  in dynamic air**

## Full Paper

### Kinetic Analysis

Non-isothermal kinetic analysis of the coordination polymers was carried out applying two different procedures: the Coats-Redfern<sup>[24]</sup> and the Horowitz-Metzger<sup>[25]</sup> methods (Figure 6-7). The kinetic and thermodynamic parameters for compounds 2 and 3 are calculated for the first step according to the above two methods and are cited in TABLE 5 and 6. The Ther-

modynamic parameters, namely entropy ( $\Delta S^*$ ), enthalpy ( $\Delta H^*$ ) and free energy ( $\Delta G^*$ ) of activation were calculated using the following standard relations:

$$\Delta S^* = R [\ln Zh / kT_s] \quad (3)$$

$$\Delta H^* = \Delta E_a \Delta RT_s \quad (4)$$

$$\Delta G^* = \Delta H^* \Delta T_s \Delta S^* \quad (5)$$

where  $h$ , Planck's constant,  $k$ , Boltzmann constant,  $R$ , gas constant and  $T_s$ , temperature at the DTG peak.

TABLE 5 : Kinetic parameters for the thermal decomposition of the coordination polymers (2-3) in dynamic air

Compound	Step	Coats-Redfern equation				Horowitz-Metzger equation			
		<u>r</u>	n	E	Z	<u>r</u>	n	E	Z
2	1 <sup>st</sup>	0.9990	0.00	28.8	5.81 x 10 <sup>2</sup>	0.9993	0.00	37.9	1.12 x 10 <sup>2</sup>
		0.9996	0.33	36.7	7.40 x 10 <sup>2</sup>	0.9998	0.33	46.2	14.6 x 10 <sup>2</sup>
		0.9998	0.50	41.5	8.35 x 10 <sup>2</sup>	0.9999	0.50	50.9	3.11 x 10 <sup>6</sup>
		0.9999	0.66	46.6	9.37 x 10 <sup>2</sup>	0.9993	0.66	39.7	8.13 x 10 <sup>5</sup>
		1.0000	1.00	57.6	11.56 x 10 <sup>2</sup>	1.0000	1.00	63.5	11.38 x 10 <sup>6</sup>
		0.9993	2.00	98.9	19.63 x 10 <sup>2</sup>	1.0000	2.00	109.7	17.40 x 10 <sup>5</sup>
3	1 <sup>st</sup>	0.9921	0.00	129.9	2.55 x 10 <sup>3</sup>	0.9930	0.00	137.8	3.71 x 10 <sup>5</sup>
		1.0000	0.33	146.5	2.95 x 10 <sup>3</sup>	0.9954	0.33	155.8	2.67 x 10 <sup>6</sup>
		0.9960	0.50	159.8	3.19 x 10 <sup>3</sup>	0.9965	0.50	165.9	8.11 x 10 <sup>6</sup>
		0.9970	0.66	167.1	3.34 x 10 <sup>3</sup>	0.9972	0.66	175.6	2.36 x 10 <sup>6</sup>
		0.9984	1.00	128.9	3.57 x 10 <sup>3</sup>	0.9946	1.00	137.5	2.14 x 10 <sup>5</sup>
		1.0000	2.00	233.8	4.66 x 10 <sup>3</sup>	1.0000	2.00	241.8	9.23 x 10 <sup>6</sup>

E in KJ mol<sup>-1</sup>, underlined  $r$  in all tables represents the best fit values of  $n$  and E

TABLE 6 : Activation parameters of the compounds (2-3) in dynamic air

Compound	Step	$\Delta S^*$	$\Delta H^*$	$\Delta G^*$
2	1 <sup>st</sup>	-196.48	24.54	100.56
3	1 <sup>st</sup>	-184.95	125.23	103.88

$\Delta H^*$  and  $\Delta G^*$  in kJmol<sup>-1</sup> &  $\Delta S^*$  in kJmol<sup>-1</sup>K<sup>-1</sup>

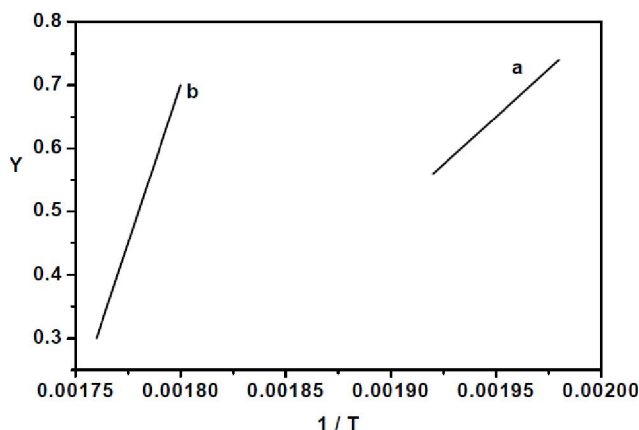


Figure 6 : Coats-Redfern plots for a) Co (II) complex and b) Cu (II) complex first step in dynamic air; where  $Y = \ln[1 - (1 - \alpha)^{1-n} / (1 - \alpha) T^2]$  for  $n \neq 1$  or  $Y = \ln[-\ln(1 - \alpha) / T^2]$  for  $n = 1$

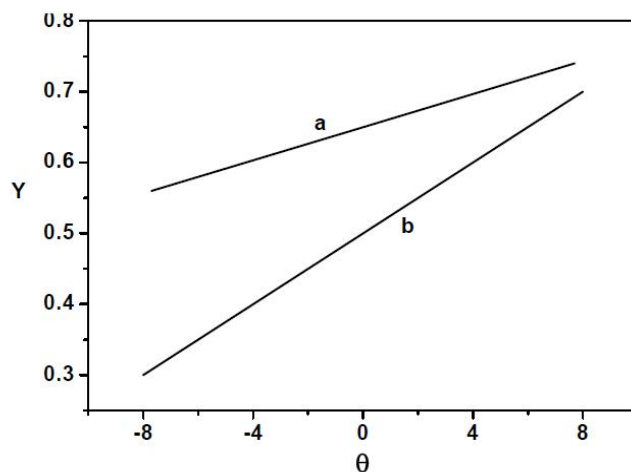


Figure 7 : Horowitz-Metzger plots for a) Co (II) complex and b) Cu (II) complex first step in dynamic air; where  $Y = \ln[1 - (1 - \alpha)^{1-n} / (1 - \alpha)]$  for  $n \neq 1$  or  $Y = \ln[-\ln(1 - \alpha)]$  for  $n = 1$

Negative  $\Delta S^*$  values for the first stage of decomposition of the Co (II) and Cu (II) coordination polymers suggest that the activated complex is more ordered than the reactants and that the reactions are slower than normal<sup>[26,27]</sup>. The more ordered nature may

be due to the polarization of bonds in the activated state, which might happen through charge transfer electronic transition<sup>[28]</sup>. The different values of  $\Delta H^*$  and  $\Delta G^*$  of the complexes refer to the effect of the type of the metal ion on the thermal stability of the complexes<sup>[29]</sup>.

### X-ray powder diffraction of the coordination polymers

The X-ray powder diffraction patterns were recorded for the coordination polymers (3) and (4). The diffraction patterns indicate that the compounds are crystalline. The crystal lattice parameters were computed with the aid of the computer program TREOR. The crystal data for the compounds belong to the crystal system triclinic. The significant broadening of the peaks indicates that the particles are of nanometer dimensions (XRD of compound (4) is depicted in Figure 8). Scherrer's equation (6) was applied to estimate the particle size of the coordination polymers:

$$D = K\lambda / \beta \cos\theta \quad (6)$$

where  $K$  is the shape factor,  $\lambda$  is the X-ray wavelength typically 1.54 Å,  $\beta$  is the line broadening at half the maximum intensity in radians and  $\theta$  is Bragg angle and  $D$  is the mean size of the ordered (crystalline) domains, which may be smaller or equal to the grain size. The crystal data together with particle size are recorded in TABLE 7. The average size of the particles lies in the range 20-34 nm for the two compounds which are in close agreement with that calculated from SEM photographs.

TABLE 7 : X-ray powder diffraction crystal data of the compounds (3-4) and their particle size

Parameters	Compound 3	Compound 4
Empirical formula	C <sub>17</sub> H <sub>22</sub> CuN <sub>4</sub> OCl <sub>2</sub>	C <sub>17</sub> H <sub>26</sub> CdN <sub>4</sub> O <sub>3</sub> Cl <sub>2</sub>
Formula weight	432.88	517.78
Crystal system	triclinic	triclinic
a (Å)	7.787	7.086
b (Å)	11.042	10.131
c (Å)	13.527	14.890
$\alpha$ (°)	62.172	58.187
$\beta$ (°)	95.871	64.297
$\gamma$ (°)	117.698	74.690
Volume of unit cell(Å <sup>3</sup> )	901.03	898.66
Particle size(nm)	20	34

### Scanning electron micrographs (SEM)

The scanning electron micrographs of copper(II) and cadmium(II) coordination polymers as representatives are given in Figures 9-10. The figures show the different morphologies of the coordination polymers. The packing of the structures on a molecular level might

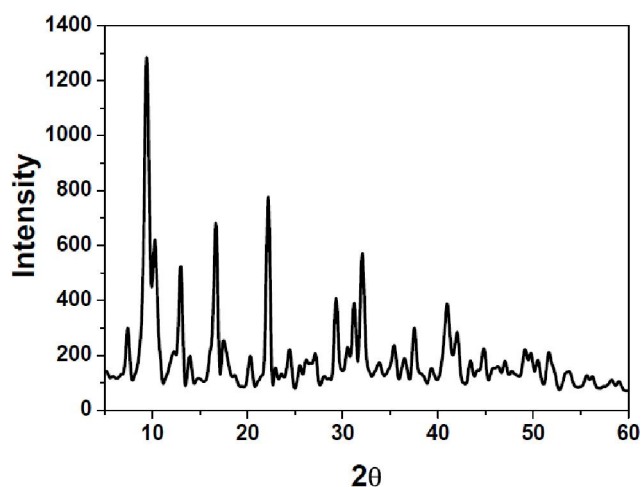


Figure 8 : X-ray of {[Cd(DPP)(MIMZ)Cl<sub>2</sub>(H<sub>2</sub>O)].2H<sub>2</sub>O}<sub>n</sub>

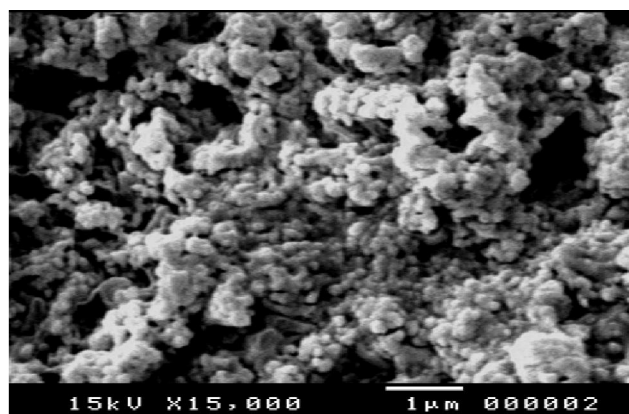


Figure 9 : S.E.M of Cu (II) coordination polymer

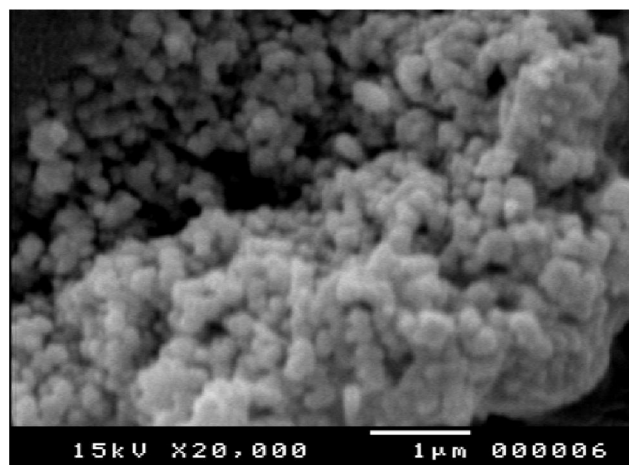


Figure 10 : S.E.M of Cd(II) coordination polymer

## Full Paper

have affected the morphology of the nano-structure of the compounds.

### Microbiological screening

The antimicrobial activity of compounds (2),(3) and (4) was tested against 5 bacterial and 6 fungal strain TABLE 8. As shown in the table compounds (2) and (4) exhibited a broad spectrum of the antibacterial action with the highest activity observed against *Bacillus cereus*

(Gram +ve). Concerning the antifungal activity, these compounds were effective against *Geotrichum Candidum* (a yeast like human pathogen fungus) with the highest inhibitory activity exerted by compound (2). *Candida albicans* (also a yeast like human pathogen fungus) was inhibited by compounds (2), (3) and (4) (Figures 11-12). It is assumed that the complexes interact mainly with bacteria and fungi through the 1-methiimidazole moiety which possesses high antibacterial and fungal effect.

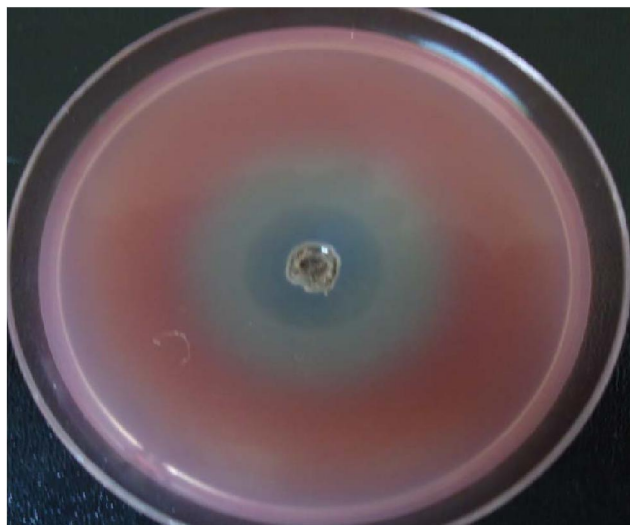


Figure 11 : Microbiological screening of compound 4 against *S.marcescens*(-ve)

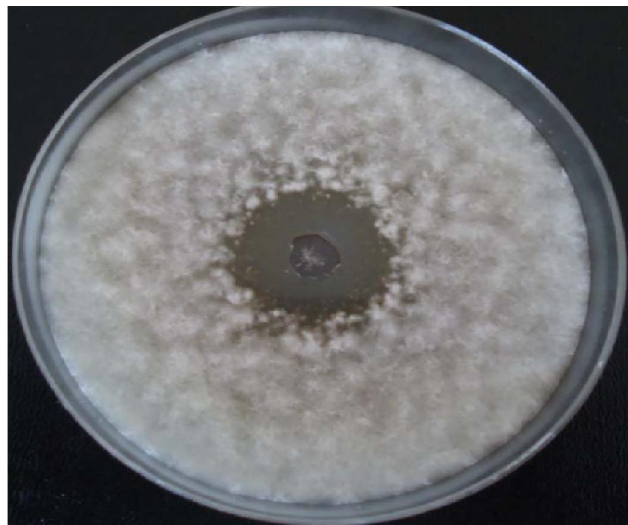


Figure 12 : Microbiological screening of compound 3 against *G.candidum*

TABLE 8 : Microbiological screening of the compounds

Compound	<i>B. Ceres</i> (G+ve)	<i>S. aureus</i> (+ve)	<i>S. Marcescens</i> (G-ve)	<i>E. coli</i> (G-ve)	<i>P. aeruginosa</i> (G-ve)	<i>T.rubrum</i>	<i>A.flavus</i>	<i>C.albicans</i>	<i>F.oxysporm</i>	<i>G.candidum</i>	<i>S.brevicaulis</i>
2	14	4	0	0	14	12	0	14	0	19	16
3	13	12	14	15	11	10	0	11	0	11	13
4	20	15	18	18	16	12	27	14	10	18	12

### ACKNOWLEDGEMENT

One of the authors (A. A. M. ALY) is very grateful to Alexander Von Humboldt Foundation for donating the magnetic susceptibility balance (MSB-Auto).

### REFERENCES

- [1] M.Fujita, Y.J.Kwon, S.Washizu, K.Ogura; *J.Am.Chem.Soc.*, **116**, 1151-1152 (1994).
- [2] O.M.Yaghi, H.Li, C.Davis, D.Richardson, T.L.Groy; *Acc.Chem.Res.*, **31**, 474-484 (1998).
- [3] J.S.Seo, D.Whang, H.Lee, S.I.Jun, J.Oh, Y.J.Jeon, K.Kim; *Nature*, **404**, 982-986 (2000).
- [4] S.Q.Ma, X.S.Wang, D.Q.Yuan, H.C.Zhou; *Angew. Chem.Int.Ed.*, **47**, 4130-4133 (2008).
- [5] K.Fromm; *Coord.Chem.Rev.*, **252**, 856 (2008).
- [6] A.Aslani, A.Morsali, M.Zeller; *Solid State Sciences.*, **10**, 1591-1597 (2008).
- [7] L.F.Marques, M.V.Marinho, N.L.Speziali; *Inorg. Chem.Acta*, **365**, 454 (2011).
- [8] M.T.Bujaci, X.Wang, S.Li, C.Zheng; *Inorg.Chim. Acta*, **333**, 152-154 (2002).
- [9] E.E.Baird, P.B.Dervan, *J.Am.Chem.Soc.*, **118**, 6141 (1996).
- [10] V.E.Borisenko, A.Koll, A.G.Rjasnyi; *J.Mol.Struct.*, **783**, 101 (2006).
- [11] K.N.Nicholson, S.A.Wood; *J.Sol.Chem.*, **31**, 703 (2003).

- [12] N.Agarwal, S.Kumar; *Ind.J.Het.Chem.*, **6**, 291 (1997).
- [13] J.Q.Liu, W.P.Wu, Y.Y.Wang, W.H.Huang, W.H.Zhang, Q.Z.Shi, J.S.Miller; *Inorg.Chim.Acta*, **362**, 1291-1295 (2009).
- [14] A.Das, C.Marchner, J.Cano, J.Baumgartner, J.Ribas; *Polyhedron*, **28**, 2436-2442 (2009).
- [15] L.Hashemi, A.Morsali, P.Retailleau; *Inorganica Chimica Acta*, **367**, 207-211 (2011).
- [16] T.Rakha; *Synth.React.Inorg.Met.Org.Chem.*, **30**, 205-224 (2000).
- [17] A.Bravo, J.Anacona; *Transition.Met.Chem.*, **26**, 20-23 (2001).
- [18] Y.T.Wang, G.M.Tang; *Polyhedron*, **26**, 782-790 (2007).
- [19] M.C.Jain, R.K.Sharma, P.C.Jain; *Gazz.Chim.Ital.*, **109**, 601 (1979).
- [20] A.B.P.Lever; *Inorganic electronic conductivity*, (2<sup>nd</sup> Edition) Elsevier Amsterdam, (1986).
- [21] A.A.El-Asmy, M.Mounir; *Trans.Met.Chem.*, **13**, 143-146 (1988).
- [22] H.B.Xiong, D.Sun, G.G.Luo, R.B.Huang, J.C.Dai; *J.Molecul.Struc.*, **990**, 164-168 (2011).
- [23] X.Zhu, H.Zhang, Y.Luo, Y.Pang, D.Tian; *Inorg. Chem.Commun.*, **14**, 562-565 (2011).
- [24] A.Coats, J.Redfern; *Nature*, **20**, 68-69 (1964).
- [25] H.Horowitz, G.Metzger; *Anal.Chem.*, **35**, 1464-1468 (1963).
- [26] G.G.Mohamed, W.M.Hosny, M.A.Abd El-Rahim; *Synth.React.Inorg.Met.Org.Chem.*, **32**, 1501-1519 (2000).
- [27] M.A.A.Beg, M.A.Qaiser; *Thermochim.Acta.*, **210**, 123-132 (1998).
- [28] K.K.M.Yusuff, A.R.Karthikeyan; *Thermochim. Acta*, **207**, 193-199 (1992).
- [29] M.E.Emam, M.Kanawy, M.H.Hafe; *J.Therm.Anal. Cal*, **63**, 75-83 (2001).